Daniel, Please copy as pdf and e-mail me a copy. You can keep the reprint Juan

Earth and Planetary Science Letters, 108 (1992) 79–92
Elsevier Science Publishers B.V., Amsterdam

[CL]

Thermal uplift and erosion across the continent–ocean transform boundary of the southern Exmouth Plateau

J.M. Lorenzo * and E.E. Vera
Lamont-Doherty Geological Observatory, Palisades, NY 10964–1090, USA

Received April 18, 1991; revision accepted October 25, 1991

ABSTRACT

Thermal evolution of the continental lithosphere at a continent–ocean transform margin is examined using a two-dimensional heat conduction model. All heating is assumed to result from the emplacement of new oceanic ridge against the continent. The assumed initial continental temperature gradient is probably best applied to regions having experienced finite-duration periods of rifting lasting tens of millions of years. A deep seismic reflection profile across the southern paleo-transform margin of the Exmouth Plateau (northwest Australia) tests the predictions of the model. Using this reflection profile, it is estimated that up to 3.5 km of sediments have been eroded from the continental rim, diminishing to almost no erosion at 60 km from the continent–ocean transform boundary. This trend and these values for erosion can be matched approximately using the model under the condition of local isostasy. A finite-difference scheme is employed, where the surface elevation is the result of the competing (1) thermal uplift (up), (2) surficial erosion (down), and (3) local isostatic rebound (up) in response to the erosion. The model predicts that most of the erosion ceases by 40 Ma after ridge emplacement and that of the order of 1000 km^3 eroded sediments are shed for every 10 km of transform length.

1. Introduction

Passive margins are commonly offset along their length by fossil transform segments [1] known as continent–ocean transform margins. These regions were first recognized for their importance in constraining the movements of separating continents, controlling the geometry of the continents and, to some degree, in defining the location of the fracture zones and oceanic transforms as their oceanward extensions [2–4].

Kinematic models of continent–ocean transform margins [5,6] usually distinguish an early stage of development in which continent–continent shearing is emphasized as the dominant process controlling the tectonic structural development of a long, narrow region in which the transform fault will eventually rupture. At a later stage as seafloor spreading proceeds, the oceanic ridge slides along the transform. Its leeward flank moves ahead of the ridge also in contact with the adjacent colder continental lithosphere. In this setting, heat conduction across the transform may induce a thermal rise above sea level and subsequent erosion of the continental side [7]. As the continental block is commonly blanketed by a sediment pile (e.g., [8,9]), the effects of erosion may remain registered as local unconformities close to the continent–ocean transform boundary [10].

A numerical geodynamic model for the evolution of continent–ocean transform margins, incorporating the effects of heat conduction across the transform has been recently proposed [11] in which observed crustal thinning across the Southwest Newfoundland continent–ocean transform margin (offshore northwest Canada) is explained by subaerial erosion of the thermally uplifted continental margin. A fundamental aspect of this model is that in addition to the heat input directly from the ridge, it can also account for the input of heat from the adjacent ridge flanks sliding past in advance of the approaching ridge. It is assumed however, that the thermal history of the

* Present address: School of Earth Sciences, Flinders University, GPO Box 2100, S.A. 5001, Australia.

oceanic lithosphere is insensitive to the presence of a colder shouldering continental block. Thus, the evolving temperature field is estimated so that at each new time step the boundary conditions are described by a simple cooling half-space model for oceanic lithosphere [12].

Few data sets exist from continent–ocean transform margins to test the general applicability of this model. Analyses of deep seismic reflection and refraction results (expanding spread profiles —ESP's) from the southern continent–ocean transform margin of the Exmouth Plateau, northwest Australia provide some support for the model by showing that several kilometers of sediments may have been removed by subaerial erosion [13]. It appears too, that additional crustal thinning may have been produced by extensional faulting across the margin, as along many rifted passive margins [14–16]. However, Lorenzo et al. [13] show that the immediately adjacent oceanic crust may have an abnormally thick lower oceanic crust which is continuous under the continental side as an underplated gabbroic wedge. The exact mechanism to explain the origin of the gabbroic unit is unclear as yet and has not been incorporated into our model. We feel these observations suggest that thermal exchange between continental and oceanic lithospheres may be responsible for the unusual crustal structure.

Here we treat the two-dimensional thermal conduction problem across a continent–ocean transform margin by developing an analytical two-dimensional analog of the plate model [17,18] for oceanic lithosphere but in which the oceanic lithosphere cools against a colder continental block. The temperature structure for a "half-plate" cooling model is used to estimate the amount of thermal uplift and ensuing subaerial erosion assuming that the lithosphere is in local isostatic equilibrium. The effects of assuming lateral strength in the lithosphere (regional isostasy) are considered for the case of a continental plate mechanically uncoupled from the subsiding oceanic lithosphere.

2. Thermal modeling

The idealized geometry of a continent–ocean transform margin system while the continental lithosphere of both plates is still touching is illustrated in Fig. 1A. A position on the continent such as X, comes first into contact with the flanks of a cooling ridge. As drifting proceeds, X encounters increasingly hotter oceanic lithosphere until the ridge arrives and joins the continent as one plate. We examine using the two-dimensional models sketched in Fig. 1 the evolution of the temperature field in the plane I–II through the ridge and continental block. In this approximation we consider that the ridge is the principal supplier of heat. A second-order contribution comes from the ridge flanks moving in advance of the ridge. As we shall see, if the ridge arrives less than a few million years after breakup, the thermal effects of the flanks are of second-order importance. This assumption reduces the number of physical parameters involved in the model and allows analytical solutions for uplift. Model parameters and physical constants used in the calculations are given in Table 1.

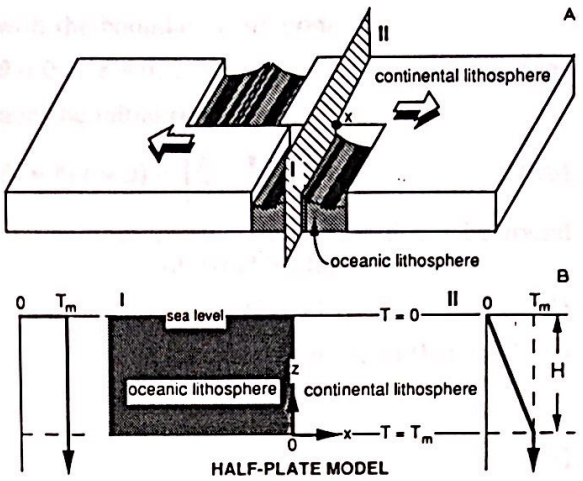

Fig. 1. (A) Block diagram of idealized ridge–transform–ridge plate boundary during development of a continent–ocean transform margin. Position X on continent is heated by progressively hotter oceanic lithosphere as ridge moves across transform fault. On arrival, ridge is emplaced permanently next to X. Half-plate model is used to examine thermal evolution of lithosphere in the plane $I-II$, after ridge abuts continent. (B) Initial and boundary conditions for half-plate cooling model through section $I-II$ in (A).

2.1. Half-plate model

The temperature field near, and at the contact between a cooling oceanic ridge and colder continental lithosphere is estimated using a simple

TABLE 1

Parameters and constants used in thermal models

Symbol	Name	Value	Units
α	volumetric thermal expansion coefficient	4×10^{-5}	$°C^{-1}$
g	gravitational acceleration	9.8	$m\ s^{-2}$
κ	thermal diffusivity	8×10^{-7}	$m^2\ s^{-1}$
ρ_c	continental crustal density	2670	$kg\ m^{-3}$
ρ_m	mantle density	3300	$kg\ m^{-3}$
ρ_w	sea water density	1000	$kg\ m^{-3}$
Y	Young's modulus	5×10^{10}	$N\ m^{-2}$
T_e	elastic plate thickness	1.5×10^{4}	m
ν	Poisson's ratio	0.25	
K	erosion constant	1.5×10^{-7}	yr^{-1}
T_m	temperature at base of lithosphere	1333	°C
H	thermal thickness of lithosphere	1.25×10^{5}	m

two-dimensional "half-plate" model (Fig 1B). At time $t = 0$, the oceanic lithosphere ($x < 0$) has a constant mantle temperature $T_0 = T_m$, and the continental lithosphere ($x > 0$), a linear temperature gradient from $T = T_m$ at its base ($z = 0$) to $T = 0°C$ at its top ($z = H$). For the simplest treatment of the problem, the contribution of radioactive sources to the temperature profile is considered minor [19]. At all times, the temperature at the base and at the top of both oceanic and continental lithosphere is kept constant at $T = T_m$ and 0°C, respectively. At $x = -\infty$, the temperature must change as that of a laterally infinite cooling plate, and at $x = +\infty$ the linear temperature gradient must remain unchanged.

The evolution of the temperature field is governed by the heat diffusion equation:

$$\frac{\partial T}{\partial t} = \kappa\left(\frac{\partial^2 T}{\partial x^2} + \frac{\partial^2 T}{\partial y^2}\right) \tag{1}$$

where κ is the thermal diffusivity that is considered constant throughout. We use non-dimensional variables:

$$x' = \frac{x}{H}, \quad z' = \frac{z}{H}, \quad t' = \frac{\kappa}{H^2}t \tag{2a}$$

$$T = T_m(1 - z' + \theta) \tag{2b}$$

$$\theta = \theta(x', z', t') \tag{2c}$$

Combining eqs. 1 and 2 and dropping the primes on the non-dimensional variables, we find:

$$\frac{\partial \theta}{\partial t} = \frac{\partial^2 \theta}{\partial x^2} + \frac{\partial^2 \theta}{\partial z^2} \tag{3}$$

with the boundary conditions:

$$\theta = 0 \text{ at } z = 0, 1; \quad t \geqslant 0 \tag{4a}$$

and the initial conditions:

$$\theta_0 = \theta(t = 0) = \begin{bmatrix} z & x < 0 \\ 0 & x > 0 \end{bmatrix} \tag{4b}$$

The appropriate solution for θ can be found by separation of variables for:

$$\theta(x, z, t) = F(x, t)G(z)J(t) \tag{5}$$

Combining eqs. 3 and 5 it is found that eq. 5 is a solution provided that:

$$\frac{\partial F}{\partial t} = \frac{\partial^2 F}{\partial x^2} \tag{6a}$$

$$\frac{1}{J}\frac{\partial J}{\partial t} = \frac{1}{G}\frac{\partial^2 G}{\partial x^2} = -k^2 \tag{6b}$$

We solve eq. 6a in terms of the error function, and 6b in terms of exponentials for J and sines and cosines for G. The boundary conditions 4a are satisfied if the amplitudes of the cosines are zero and $k = n\pi$, $n = 1,2,3,\ldots$ The solution for θ that satisfies the boundary condition can then be written as:

$$\theta = \frac{1}{2}\operatorname{erfc}\left(\frac{x}{2\sqrt{t}}\right) \sum_{n=1}^{\infty} A_n\, e^{-n^2\pi^2 t} \sin n\pi z \tag{7}$$

where $\operatorname{erfc}(u) = 1 - \operatorname{erf}(u)$ is the complementary error function.

At $t = 0$ we find that:

$$\theta_0 = \begin{bmatrix} \sum_{n=1}^{\infty} A_n \sin n\pi z & x < 0 \\ 0 & x > 0 \end{bmatrix} \tag{8}$$

Thus the initial conditions 4b are satisfied if the sum in eq. 8 is z; this requires:

$$A_n = \frac{2(-1)^{n+1}}{n\pi}$$

The solution for θ is:

$$\theta = \frac{1}{2}\operatorname{erfc}\left(\frac{x}{2\sqrt{t}}\right) + \frac{2}{\pi}\sum_{n=1}^{\infty}\frac{(-1)^{n+1}}{n} e^{-n^2\pi^2 t} \sin n\pi z \tag{9}$$

The temperature distribution is obtained by combining eqs. 2 and 9. For $x = -\infty$, $\operatorname{erfc}(x/2\sqrt{t}) = 2$

at all times and the temperature evolves exactly as that of a one-dimensional cooling plate model (e.g., [12,18]). For $x = +\infty$, $\mathrm{erfc}(x/2\sqrt{t})$ becomes zero and the initial linear temperature gradient remains unchanged with time.

In the region of contact between the two half-plates, horizontal temperature gradients are significant and the oceanic lithosphere loses heat not only through vertical conduction but also laterally into the continental lithosphere. The resulting perturbation to the initial linear temperature gradient on the continental side is:

$$\Delta T(x, z, t) = T - T_0 = T_m\theta, \quad x > 0 \qquad (10)$$

The change in the density distribution is due to the effects of thermal expansion, estimated by:

$$\rho(T) = \rho(T_0)[1 - \alpha\Delta T(x, z, t)]$$

where α is the volumetric thermal expansion coefficient.

Assuming that the lithosphere has no lateral strength and rests in isostatic equilibrium in the upper mantle, then the vertical changes in the density structure are compensated by adjustments to the surface elevation of the half plate. For $x > 0$, we consider that the top of the continental lithosphere is initially at sea level, so that the

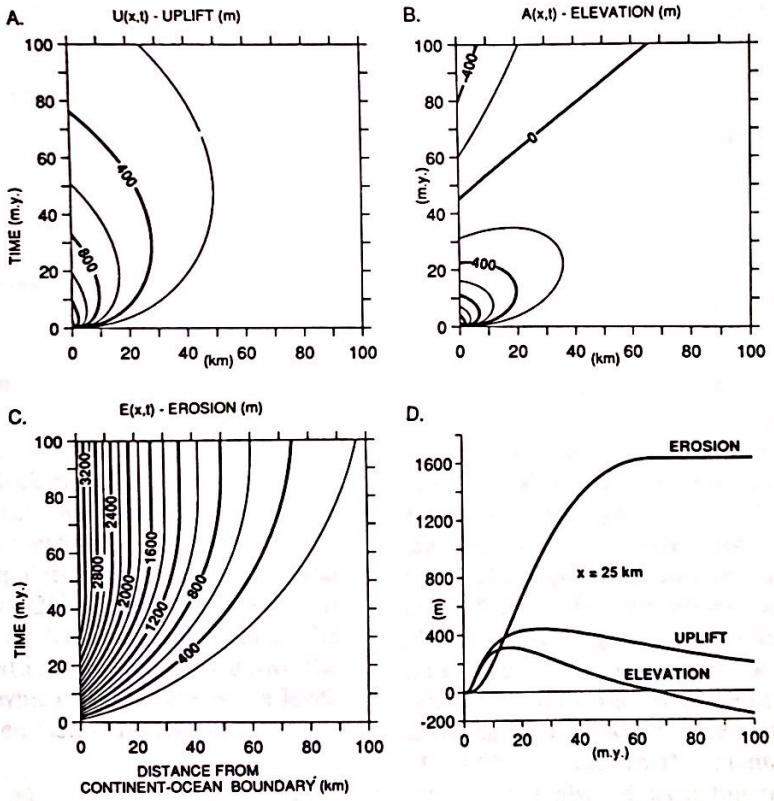

Fig. 2. Contour plots of uplift, elevation and erosion as a function of distance from continent–ocean boundary and millions of years after initial ridge–continent contact for half-plate model. Contours in this figure and Figs. 3 and 8, result from a cubic spline interpolation through points of a 1 Ma by 1 km grid calculated using parameters in Table 1. (A) Values for thermal uplift (U) are calculated using eq. 12 from half-plate model. U is produced by thermal expansion of lithosphere in vertical direction and readjustment of its base under conditions of local isostatic equilibrium. (B) Elevation (A) is a product of (1) thermal uplift, (2) erosion of surface, and (3) isostatic rebound of continental lithosphere because of erosional unloading. As thickness of lithosphere is reduced through erosion, surface eventually comes to rest several hundreds of meters below sea level. (C) Time accumulated erosion estimates can be 3–4 times larger than maximum elevation value. (D) Overplot of cross-sections through (A), (B) and (C) at a common distance of 25 km.

consequent uplift, $U(x, t)$, will be:

$$U(x,t) = \alpha \int_0^H \Delta T(x, z, t)\, dz, \quad x > 0 \qquad (11)$$

One third of the rise is due to thermal expansion in the vertical direction and two thirds to uplift of the base of the lithosphere in response to local isostatic readjustment. Substituting eq. 10 into eq. 11 and after integration, we obtain:

$$U(x,t) = T_m H \alpha \frac{1}{2} \operatorname{erfc}\left(\frac{x'}{2\sqrt{t'}}\right) \frac{4}{\pi^2} \times \sum_{n=0}^{\infty} \frac{e^{-(2n+1)^2\pi^2 t'}}{(2n+1)^2}, \quad x > 0. \qquad (12)$$

From eq. 11 on, we return to our initial convention of simple and primed variables to indicate dimensional and non-dimensional variables, respectively. Figure 2A shows a contour plot calculated using eq. 12. For a given distance, U gradually increases from zero to a maximum value that is reached at a time (in Ma) that is roughly numerically equal to distance (in km). After this time, U starts decreasing asymptotically towards zero (sea level) as the heat provided by the ridge diffuses and the original linear temperature gradient is recovered.

2.2. *Subaerial erosion*

In our models, $U(x, t) > 0$ implies that the top of the continental block rises above sea level and that erosion may ensue. We estimate the amount of total accumulated erosion $E(x, t)$ (denudation) using the formulation of Ahnert [20] and Pitman and Andrews [21]. They have shown that the rate of erosion, $\partial E/\partial t$, is proportional to the average elevation, $A(x, t)$, of a locality above the eroding base level, which in this case is sea level. This formulation then yields the relation:

$$\frac{\partial E(x,t)}{\partial t} = KA(X,t) \qquad (13)$$

where K is the constant of erosion, determined empirically.

In order to integrate eq. 13 to find E, however, a relationship between E, A and U must first be established. To do this we assume local isostatic equilibrium at all times. The final elevation is the result of several competing mechanisms, namely: (1) thermal uplift that raises the continental block above sea level ($+U$); (2) erosion that lowers the surface of the uplifted continent ($-E$); and (3) isostatic rebound of the continental lithosphere in response to erosional unloading ($+E\rho_c/\rho_m$) where ρ_c is the density of the crust being eroded and ρ_m is the mantle density. For $\rho_c = 2670$ kg/m^3 and $\rho_m = 3300$ kg/m^3 (Table 1), this rebound is approximately 80% of the eroded thickness. Thus in terms of the thermal uplift and total accumulated erosion E, the final elevation A is:

$$A(x,t) = U(x,t) - \frac{\rho_m - \rho_c}{\rho_m} E(x,t). \qquad (14)$$

Equation 14 assumes that thermal uplift is not modified by erosion, that is, U is simply computed using eq. 12. Strictly speaking, erosion changes the lithospheric thickness and hence the temperature structure and uplift. These changes, however, are of the order of 1% or less representing only second-order effects that are unimportant in the context of this paper.

Combining eqs. 13 and 14 leads to an elementary linear differential equation for E that can be readily solved in terms of a time integral that involves the known uplift function U. In practice, however, it is simpler to directly integrate eq. 13 numerically. We have used a straightforward finite difference scheme with a time increment value Δt of 100,000 yrs; smaller time increments always yielded almost identical results. The integration process is started with $E = A = U = 0$ at $t = 0$. The right-hand side of eq. 13 is calculated and a finite difference version of eq. 13 is used to obtain $E(\Delta t)$. Equation 14 is then used to compute $A(\Delta t)$ (U is obtained from eq. 12) which is reinserted into the right-hand side of eq. 13, allowing for time to advance and the computation of $E(2\Delta t)\ldots$ etc. In this manner we obtain not only E, but also A as a function of time for a given distance x; the process must be repeated for every desired x. Figure 2B shows a contour plot of $A(x, t)$, the elevation, and Fig. 2C of $E(x, t)$, the erosion. In our calculations, erosion takes place as long as the surface of the continent is above sea level ($A > 0$). Below this level, the continent is under water and there is no erosion.

The time–distance boundary for the end of erosion is marked by a straight 0-m elevation contour in Fig. 2B or, equivalently in Fig. 2C, at those places where the erosion contours first become parallel to the time axis. In the integration process, the lack of erosion is introduced by simply setting $K=0$ if $A<0$, and the fact that the continent is submerged by modifying A to $A\rho_m/(\rho_m-\rho_w)$ (ρ_w = sea-water density) in order to introduce an isostatically compensated sea-water column.

The temporal evolution of variables U, E and A can be examined by comparing their behavior at a common distance from the continent–ocean transform boundary (Fig. 2D). At a distance of 25 km, a maximum value for erosion of 1629 m is reached at ~65 Ma (elevation = 0), although more than 80% of the erosion is accomplished by ~40 Ma. Because of erosion, the elevation is always less than or equal to the predicted thermal uplift, and local maximum elevation is attained at least 10 Ma before the maximum thermal pulse arrives. Without erosion, the surface of the lithosphere would subside asymptotically towards sea level but because of erosion, the surface eventually comes to rest below sea level.

2.3. *Limitations of thermal modeling*

Continent–ocean transform margins develop along passive margins. Passive margins are widely regarded to form through thinning of the lithosphere either over a finite period of time lasting tens of millions of years (e.g., [22]) or practically instantaneously (e.g., [19]). The thermal effects of our model are sensitive to the initial thermal thickness of the continental lithosphere (12) and are therefore dependent on the previous rifting history. A thinner lithosphere reduces the horizontal thermal gradient, diminishing inflow of heat from the abutting oceanic lithosphere and attenuating the amount of uplift and erosion. However, if the lithosphere is thinned over a finite period of time, more heat can diffuse during rifting than predicted by the instantaneous stretching models. Consequently, at the initiation of seafloor spreading, the continental temperature gradient would be closer to that of the initial non-rifted continent and the thermal thickness of the lithosphere would be greater. Predictions of the half-plate model are favored by long rifting periods of time, lasting tens of millions of years.

In estimating uplift and erosion we have treated the lithosphere as having no flexural rigidity so that the temperature-induced density changes are compensated locally by vertical displacements of the lithosphere. It follows that there should be no flexural coupling across the transform as the lithosphere is infinitely weak. This view is supported by available geophysical data sets which show that the maximum extent of erosion occurs in the proximity of the continent–ocean transform margin [11,23]. By analogy to oceanic fracture zone studies (e.g., [24]) even for a small initial continental elastic thickness of ~15 km at the moment of ridge contact, the effect of mechanical coupling would be to pull the continental side down and displace the position of maximum uplift/erosion of the order of 10 km away from the continent–ocean transform boundary. Admittance function studies from across the Southwest Newfoundland Fracture Zone also conclude that the mechanism for compensation at the transform suture is by local isostasy [25].

Whereas mechanical coupling across the continent–ocean transform margin may not dominate during its evolution, the continental lithosphere could still behave elastically, away from the boundary, without breaching the observational constraints outlined above. This is the case of a free-end plate or "broken half-plate" model which, while mechanically uncoupled from the oceanic side, rises the greatest amount closest to the heat source at the contact between the two plates. By assuming that the lithosphere has non-zero flexural rigidity, the temperature-induced density changes will be compensated by a reduced uplift, but distributed over a broader region than in the Airy isostatic case. Like many investigators of fracture zone evolution (e.g., [26–29]), we treat the lithosphere as a thin two-dimensional elastic plate. The differential equation that describes the flexural response of such a plate to loading (P) is:

$$P(x,t)=D\frac{\partial^4 y(x,t)}{\partial x^4}+g\rho_m y(x,t) \qquad (15)$$

where y is the vertical displacement of the base of the lithosphere and g is the gravitational ac-

celeration. D, the flexural rigidity, treated as constant, is given by:

$$D = \frac{YT_e^3}{12(1-\nu^2)}$$

where Y is Young's modulus, T_e is the effective elastic thickness of the lithosphere and ν Poisson's ratio. In our case, loading (P, units of pressure) is directed upwards at the base of the elastic plate, produced by the buoyancy force due to the thermal expansion and which can be expressed as:

$$P(x,t) = \tfrac{2}{3}\alpha g \rho_m \int_0^H \Delta T(x,z,t)\,\mathrm{d}z, \quad x>0$$

As the base rises, the vacated space is occupied by the fluid substrate which supplies an upward directed restoring force, represented by the second term on the right of eq. 15.

We solve eq. 15 considering that there is no mechanical coupling across the fracture zone. The non-coupling condition can be fulfilled treating the continental side as a semi-infinite beam with a free end. We derive the necessary end-conditioning forces to create a broken plate as proposed by Hetenyi ([30], p. 22). The total rise of the top of the lithosphere will consist of a flexural component and a component due to the thermal expansion:

$$U(x,t) = y(x,t) + \tfrac{1}{3}\alpha \int_0^H \Delta T(x,z)\,\mathrm{d}z, \quad x>0 \qquad (16)$$

When $T_e = 0$ and hence $D = 0$ in eq. 15, the lithosphere does not have horizontal strength and eq. 16 becomes identical to eq. 11 for the half-plate model in local isostatic equilibrium.

Apparently the rift transects of many passive margins exhibit an elastic thickness that lies between 5 and 10 km [25,31–34]. Figure 3 displays the results of calculating the thermally induced flexural uplift using eq. 16. Even for an elastic thickness of 15 km (Table 1), the predicted values are very similar to the "half-plate" Airy case of 0 elastic thickness implying that the local isostatic approximation is appropriate for a first-order treatment of the problem.

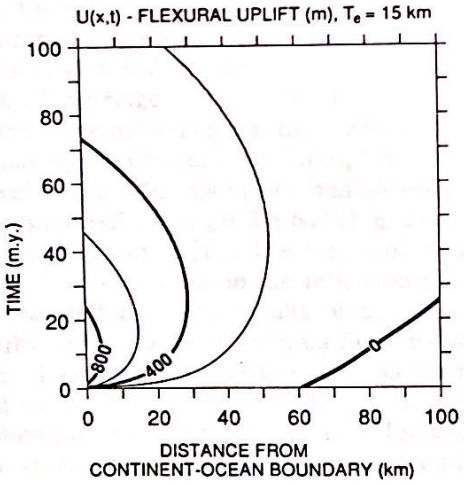

Fig. 3. Contour plot of flexural uplift as a function of distance from continent–ocean boundary and millions of years after initial ridge–continent contact for a broken plate model with an effective elastic thickness (T_e) of 15 km; see Table 1 for other parameters. There is a shallow moat developed beyond ~60 km, but at smaller distances, contour pattern is very similar to Airy case of Fig. 2C.

3. Southern Exmouth Plateau, an example of a continent–ocean transform margin

3.1. Seismic reflection data

Thermal models that explain the evolution of continent–ocean transform margins are still in a preliminary stage of testing as there is little structural or stratigraphic information available with which to make comparisons. Acoustic profiles across such margins have in general only been able to image the topmost portion of the pre-rift basement on the continental side [8–10,35] and not the structure of the adjacent oceanic crust. With the exception of the Southwest Newfoundland continent–ocean transform margin [36–38], only a recent seismic study of the southern Exmouth Plateau, northwest Australia (Fig. 4) provides as complete a structural profile across a continent–ocean transform margin [13].

The southern Exmouth Plateau forms part of a broad starved passive margin which experienced rifting in the Middle–Late Jurassic [39–41]. Seafloor spreading did not commence in the surrounding basins until at least anomaly M10 time [42] in the Early Cretaceous (~130 Ma; [43]).

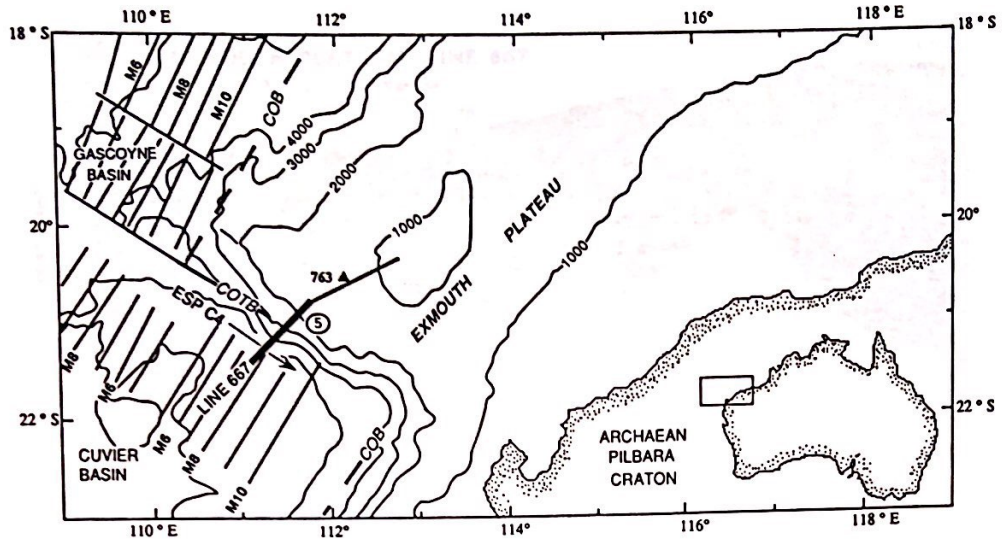

Fig. 4. Bathymetric map of central and southern Exmouth Plateau (northwest Australia) study area with isobaths drawn every 1000 m. Ship track for seismic reflection Line 667 (thin straight line) crosses from center of plateau through paleo-transform margin and into oceanic crust. Thick line segment refers to that portion of seismic profile discussed in text and seen in Fig. 5 (circled number). Expanding spread profile (ESP C4) was shot almost at right angles to Line 667 over oceanic crust and in direction shown by arrow. Solid triangle locates ODP Site 763, 1 km northwest of Line 667. Continent–ocean boundary (COB), continent–ocean transform boundary (COTB) and magnetic isochrons (M10, M9, etc.) come from Fullerton et al. [53].

Part of the available seismic reflection profile is shown in Fig. 5 and was gathered along Line 667 (Fig. 4) imaging both continental crust, and oceanic crust of approximately M8 age (~ 128 Ma). From the relative positions of the magnetic isochrons we can deduce that this portion of the continental rim first came into contact with the flank of the ridge at about M9 time (~ 129 Ma). As the ridge moved closer, the area encountered increasingly hotter oceanic lithosphere until the arrival of the ridge about one million years later.

Seismic reflection profile 667 (Fig. 5) is taken from Lorenzo et al. [13]. The nature of the major tectonic–seismic units in the reflection profile is extrapolated from the results of drilling at the nearby Ocean Drilling Program Site 763 [44] located 1 km northwest of Line 667, 55 km northeast of CDP 5000 (Fig. 4). Along Line 667, the faulted pre-rift basement consists of Triassic shallow-water reefal limestones and associated sediments. Resting unconformably above, lies a "syn-rift" sequence of shallow-water terrigenous sediments (about 1 km thick) of Tithonian–Valanginian age (~ 150–130 Ma). This sequence is in turn truncated by an erosional hiatus that spans the Barremian–Hauterivian (~ 130–119 Ma). An onlapping "post-rift" sequence comprising about 1 km of hemi-pelagic to eupelagic Aptian–Recent carbonate oozes (~ 119–0 Ma) caps the sedimentary package.

3.2. *Estimates of crustal thinning*

Between CDP 5000 and the continent–ocean transform boundary to the south, the pre-rift and syn-rift sections diminish in overall thickness (Fig. 5). We postulate that these variations in thickness may be explained by thermal uplift and erosion of the continent–ocean transform margin during drifting. North of CDP 5000, the seafloor becomes horizontal and the post-rift section suffers little diminution in thickness attributable to erosion (Fig. 3 in [45]). We can thus use the section at CDP 5000 as a reference against which the remaining sections can be compared—the difference can be attributed to erosion. We have established, as standard for comparison, the distance between the seafloor and the first high-amplitude reflector below the top of the Triassic pre-rift basement. This lower boundary probably corresponds to a shallow detachment surface which

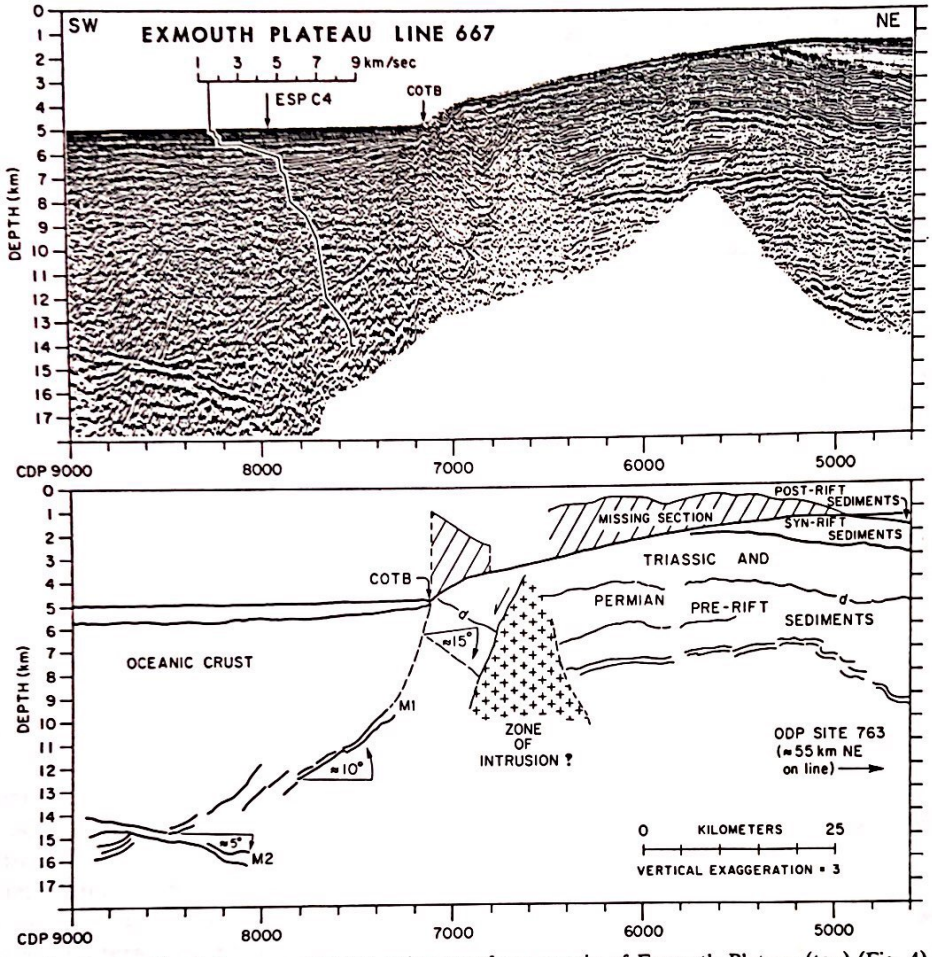

Fig. 5. Seismic reflection profile shot across southern paleo-transform margin of Exmouth Plateau (top) (Fig. 4), accompanied below by corresponding line-drawing interpretation. Profile has been depth-converted using velocity–depth solutions obtained from analysis of expanding spread profiles (ESP's), shot perpendicular to CDP Line 667 [13]. Velocity vs. depth solution derived from analysis of one such ESP (C4) in oceanic crust is superimposed on seismic section.

parallels the sedimentary reflectors [13] and was chosen because it is an easily distinguishable and laterally continuous reflector. The difference between the standard and the thickness measured orthogonally between the two reference horizons at any point is then ascribed to denudation. Values of denudation were calculated every 2.5 km, or equivalently, every 100 CDP's and are plotted in Fig. 6. In Fig. 6 we have overlaid the calculated amounts of erosion using the half-plate thermal model integrated to 40 Ma.

The cut-off time for integration of 40 Ma is constrained geologically by the nature of the post-rift sediments. As long as the continental rim lies above sea level, the eroded sediments could become incorporated into the post-rift sedimentary body. If so, the end of erosion could be marked by a change in the sedimentary facies. Haq et al. [44] note a disappearance of the terrigenous component in the post-rift sediments at the Cenomanian/Turonian transition over all of the southern Exmouth Plateau. This occurred approximately 40 Ma after the ridge was emplaced in our area of study (isochron M8). According to the half-plate model example in Fig. 2D, by 40 Ma most of the erosion is complete. We can arrive at a more general but similar conclusion by calculating the total area of eroded section out to large distances through time, as seen in Fig. 7. By including all distances even as

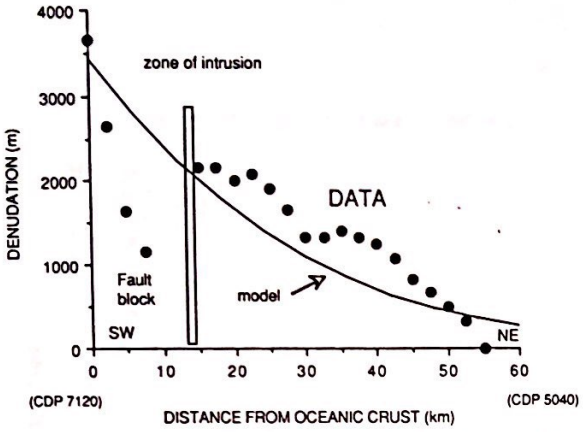

Fig. 6. Observational (dots) and theoretical estimates of denudation (continuous line) as a function of distance from continent–ocean boundary derived from reflection profile of Line 667 (Fig. 5) and calculations with half-plate model (Fig. 2), respectively. Model was run for a period of 40 Ma.

far as 100 km from the continent–ocean transform boundary, the estimated maximum possible area of eroded material is approximately 110 km^2 and almost ~75% of this value is reached within ~40 Ma. For every 10 km of transform length, these estimates imply that of the order of 10^3 km^3 of eroded sediment could be shed from the elevated rim. The facies change could be a regional phenomenon however, as Veevers and Johnstone [46] recognized it as a feature of the sedimentation patterns occurring along all of the western Australian margin from 15° to 35°S.

The apparent values for denudation increase southward until about CDP 6400, where the planar-parallel reflection facies in the pre-rift portion terminates abruptly against a wedge-shaped region of chaotic reflection patterns. Mutter et al. [45] interpret similar features on the western margin of the Exmouth Plateau as igneous intrusions. They are usually present within ~30 km from the continent–ocean boundary and presumably imply that extension occurred across the transform.

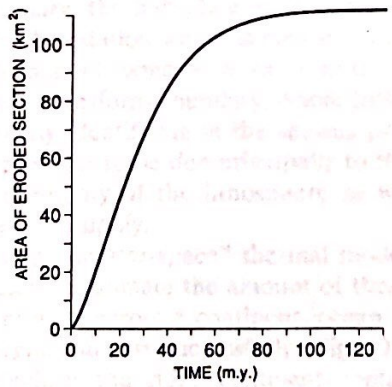

Fig. 7. Plot of total area of eroded section out to distances of 100 km from continent–ocean transform boundary for half-plate model, as a function of time after ridge–continent contact.

Between the chaotic reflection wedge and the oceanic crust, the basement reflectors become more laterally discontinuous and dip northwards ~15°. We suggest this was caused by localized fault-block rotation during extension across the margin. On the northern side of the block, the amount of estimated denudation is significantly smaller (Figs. 5 and 6), perhaps because faulting took place prior to erosion and sheltered the sediments.

By comparison, north of the chaotic reflection wedge the structural style is distinctly different. The pre-rift basement is folded and dissected by high-angle normal and reverse faults with a variable vergence ("flower structures"), some of which can be followed even to depths of 10 km (Fig. 5, CDP 4800). This structural character is typical of strike-slip deformation zones and is markedly different to the dominant extensional geometric styles seen at rifted basins [47–49]. Crustal thickness estimates at the same distance from the rifted continent–ocean boundary in the center of the plateau indicate that extensional factors are ~150% [45]. We have not been able to determine the crustal thickness seismically near this rotated block but, using a standard 30 km thick continental crust as reference in conditions of local isostasy, the great depth at which this block lies, implies a thinner continental crust and greater extension factors. Todd and Keen [11] identify a narrow zone, 25 km wide, along the southern Newfoundland continent–ocean transform margin in which the crust thins from 8 to 20 km but they attribute the attenuation of the crust wholly to subaerial erosion.

4. Discussion

Several thousands of meters of sediments are apparently missing along the southern Exmouth rim (Fig. 6), with respect to the adjacent plateau.

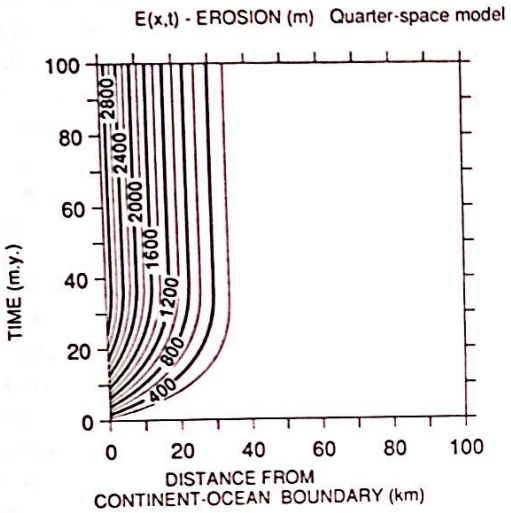

Fig. 8. Contour plot of erosion as a function of distance from continent–ocean boundary and millions of years after initial ridge–continent contact for quarter-space model, using numerical technique described in text. Comparison with erosion for half-plate model (Fig. 2C) shows similar results for less than ~10 Ma. Afterwards, however, top of quarter-space continues to subside indefinitely, eventually falling below sea level so that at ~40 Ma and at all distances erosion ceases.

Irrespective of the many inherent limitations of thermal modeling [11], our study suggests that the trend and order of magnitude of the observed values of erosion obtained from the study of the reflection profile are closely matched by the half-plate model. At the continent–ocean transform boundary, the half-plate model predicts ~3500 m of denudation which decreases to almost zero at distances beyond ~60 km from the continent–ocean transform boundary, where little erosion is clearly identifiable in the seismic profiles. We interpret this to be due principally to the low thermal diffusivity of the lithosphere as well as the finite heat supply.

A cooling "quarter-space" thermal model can also be used to estimate the amount of thermally induced erosion across a continent–ocean transform margin, but less successfully (Fig. 8). This model idealizes the ridge–continent contact as the juxtaposition of two infinite quarter spaces and has been used repeatedly in oceanic fracture zone studies [24,50–52]. At time = 0, the temperature distribution is identical to that of the plate model. However, at time > 0 the depth to the base of the thermal lithosphere increases indefinitely because the lower boundary constraint is $z = -\infty$, $T = T_m$, whereas in the half-plate model the temperature at the base of the lithosphere is kept constant. In general, the trend of the predicted values parallel the data but are smaller than the predictions of the half-plate model by ~1000 m.

Several causes can explain a second-order difference of ~500 m that exists between the theoretical determinations using the half-plate model and the seismic observations (Fig. 6). Some of the parameters used in the modeling could be varied to fit the data more closely such as K; the erosion constant may have been larger in the geologic past depending on the climate and rock type being eroded. Additional uplift and erosion could have been provided by the heat from the flanks of the approaching ridge. From Fig. 1 we can deduce that the period of time this heating event lasts, depends on the rate at which the ridge moves along the transform and the distance it must travel to arrive at any given point. In our case, the continent was in contact with young oceanic lithosphere (less than 1 Ma old), for ~1 Ma before the ridge abutted (slip rate ~3.2 cm/yr [53]). The accumulated erosion could amount to an additional few hundred meters (Fig. 2C) and perhaps explain the difference between the observations and the predictions of the model. We note that the predictions of our model may represent a low-end extreme of possible thermal effects and that for a given offset, faster slip rates would tend to further increase these effects [11].

Near our study area, the crustal extension factors are approximately 150%. Using the quarter-space model as a simple guide, we estimate that a lithosphere thinned by the same amount would decrease the maximum amount of erosion by about half. However, during the long rifting history that lasted from the Middle Jurassic until the start of seafloor spreading in the early Cretaceous, the continental lithosphere may have had sufficient time (~50 Ma) to thermally equilibrate to the initial conditions of our model. For a 50 Ma rifting phase, the post-rift subsidence may decrease by as much as 50% over the predictions of less realistic instantaneous rifting models [22].

In fact, the syn-rift sediments were very near sea level at the beginning of drifting [44]. We propose that because of the attenuated post-rift subsidence, the thermal consequences of ridge emplacement would not deviate substantially from the predictions of our models, namely up to several thousands of meters of erosion, increasing towards the continent–ocean boundary.

According to our model, ~1400 m of uplift can be expected close to the margin within a few million years after the initiation of heating. These predictions may be tested to some degree in other geological settings. For example, lateral heat conduction can induce uplift of the unthinned continental lithosphere adjacent to rift valleys. In the Gulf of Suez region, at least 1 km of rift flank uplift has taken place since rifting began ~20 Ma [54]. Half the present-day uplift can be explained by conductive effects [55]. Although the different tectonic setting and smaller lateral temperature gradients may be responsible for the smaller rates of uplift, the continental lithosphere experiences substantial thermal uplift.

Continent–ocean transform margins may also be affected by mass wasting which could cause submarine erosion of the continent–ocean transform rim. Along the Guayamas continent–ocean transform margin in the Gulf of California [56], mass wasting has eroded the transform ridge and contributed to thickening the adjacent basin deposits at the base of the slope. Corresponding to the region of the interpreted fault block in the seismic profile of Line 667, Exon and Willcox [57] have suggested that a zone of slumping occurs along the lower continental slope of the southern Exmouth Plateau between depths of ~3000–4800 m. Their slumped sequence is characterized by a blanketing chaotic reflection facies with a hummocky seafloor surface and whose thickness increases toward the toe of the slope. Our seismic profile does not seem to exhibit these features. The chaotic facies wedge that is present interrupts the sedimentary reflectors along a very steep interface and down to depths of 10 km or more.

5. Conclusions

Crustal thinning at continent–ocean transform margins may be produced by extensional faulting and thermally induced subaerial erosion. A simple half-plate heat conduction model that envisages ridge heating of juxtaposed continental lithosphere is used to explain erosion of up to 3500 m of missing sediments along the southern Exmouth continent–ocean transform margin, northwest Australia.

Interpretation of seismic reflection data suggests that the maximum degree of erosion occurs in the proximity of the continent–ocean boundary and so a local isostatic assumption appears sufficient for a first-order treatment of the problem. After the ridge is emplaced, oceanic lithosphere cools through vertical as well as lateral conduction of heat into the colder continental block. We propose that the protracted rifting history which lasted perhaps as long as 50 Ma, favors the half-plate model because it gave the continent time to equilibrate thermally and acquire a thermal gradient that was close to the pre-rift state and hence also close to the initial conditions set by our model. Second-order discrepancies of a few hundred meters between the predicted estimates for erosion of the model and the data may be due to the thermal effects of the ridge flanks which were not considered in the modeling.

Theoretical results from the half-plate model imply that almost 75% of the erosion is accomplished within the first 40 Ma of thermal evolution and that of the order of 1000 km^3 of sediments are shed for every 10 km of transform length. As well, because of erosion, the surface elevation is always less than or equal to the predicted thermal uplift and the maximum elevation is attained before the arrival of the maximum thermal pulse. Hence, surface elevation is only an approximate indicator of the stage of thermal evolution.

Acknowledgements

We are grateful to J.C. Mutter, J. Mascle and two anonymous reviewers for providing perceptive comments that helped improve the manuscript. We give special thanks to J. Graney for invaluable logistical support. This project was supported by the National Science Foundation under Grant No. OCE 84–10130 and by the Industrial Associates of the Lamont-Doherty Geological Observatory. Lamont-Doherty Geological Observatory Contribution No. 4835.

References

1 J.T. Wilson, A new class of faults and their bearing on continental drift, Nature 207, 343–347, 1965.

2 X. Le Pichon and D.E. Hayes, Marginal offsets, fracture zones and the early opening of the South Atlantic, J. Geophys. Res. 76, 6283–6293, 1971.

3 X. Le Pichon and P.J. Fox, Marginal offsets, fracture zones and the early opening of the north Atlantic, J. Geophys. Res. 76, 6294–6308, 1971.

4 J. Francheteau and X. Le Pichon, Marginal fracture zones as structural framework of continental margins in south Atlantic Ocean, A.A.P.G. Bull. 56, 991–1007, 1972.

5 R.A. Scrutton, On sheared passive continental margins, in: Crustal Properties Across Passive Margins, C.E. Keen, ed., pp. 293–305, Elsevier, Amsterdam, 1979.

6 J. Mascle and E. Blarez, Evidence for transform margin evolution from the Ivory Coast–Ghana continental margin, Nature 326, 378–381, 1987.

7 R.A. Scrutton, Crustal structure and development of sheared passive continental margins, in: Dynamics of Passive Margins, Geodynamics Series V. 6, R.A. Scrutton, ed., pp. 133–140, American Geophysical Union, Washington, D.C., 1982.

8 S. Robson and R. Dingle, A GLORIA traverse over the marginal fracture zone and the continental margin of SE Africa, Mar. Pet. Geol. 3, 31–36, 1986.

9 J. Mascle, D. Mougenot, E. Blarez, M. Marinho and P. Virlogeux, African transform continental margins: examples from Guinea, the Ivory Coast and Mozambique, Geol. J. 22, 537–561, 1987.

10 J.M. Lorenzo and J.C. Mutter, Seismic stratigraphy and tectonic evolution of the Falkland/Malvinas Plateau, Rev. Bras. Geoc. 18, 191–200, 1988.

11 B.J. Todd and C.E. Keen, Temperature effects and their geological consequences at transform margins, Can. J. Earth Sci. 26, 2591–2603, 1989.

12 B. Parsons and J.G. Sclater, An analysis of the variation of ocean floor bathymetry and heat flow with age, J. Geophys. Res. 82, 803–827, 1977.

13 J.M. Lorenzo, J.C. Mutter, R.L. Larson, P. Buhl, J.B. Diebold, J. Alsop, R. Mithal, J. Hopper, D. Falvey, P. Williamson and F. Brassil, Development of the continent–ocean transform boundary of the southern Exmouth Plateau, Geology 19, 843–846, 1991.

14 A.H. Stride, J.R. Curray, D.G. Moore and R.H. Belderson, Marine geology of the Atlantic continental margin of Europe, Philos. Trans. R. Soc. London 264, 31–75, 1969.

15 O. DeCharpal, P. Guennoc, L. Montadert and D.G. Roberts, Rifting, crustal attenuation and subsidence in the Bay of Biscay, Nature 275, 706–711, 1978.

16 J.A. Grow, R.E. Mattick and J.S. Schlee, Multichannel seismic depth sections and interval velocities over outer continental shelf and upper continental slope between Cape Hatteras and Cape Cod, in: Geological and Geophysical Investigations of Continental Margins, AAPG Mem. 29, J.S. Watkins, L. Montadert and P.W. Dickerson, eds., pp. 65–83, American Association of Petroleum Geologists, Tulsa, Okla., 1979.

17 M.G. Langseth, X. Le Pichon and M. Ewing, Crustal structure of mid-ocean ridges, 5, Heat flow through the Atlantic Ocean floor and convection currents, J. Geophys. Res. 71, 5321–5355, 1966.

18 D.P. McKenzie, Some remarks on heat flow and gravity anomalies, J. Geophys. Res. 72, 6261–6273, 1967.

19 D.P. McKenzie, Some remarks on the development of sedimentary basins, Earth Planet. Sci. Lett. 40, 25–32, 1978.

20 F. Ahnert, Functional relationships between denudation, relief and uplift in large mid-latitude drainage basins, Am. J. Sci. 270, 243–263, 1970.

21 W.C. Pitman and J.A. Andrews, Subsidence and thermal history of small pull-apart basins, in: Strike-Slip Deformation, Basin Formation, and Sedimentation, K.T. Biddle and N. Christie-Blick, eds., Soc. Econ. Paleontol. Mineral., Spec. Publ. 37, 45–49, 1985.

22 J.R. Cochran, Effects of finite rifting times on the development of sedimentary basins, Earth Planet. Sci. Lett. 66, 289–302, 1983.

23 I. Reid, Effects of lithospheric flow on the formation and evolution of a transform margin, Earth Planet. Sci. Lett. 95, 38–52, 1989.

24 D.T. Sandwell and G. Schubert, Lithospheric flexure at fracture zones, J. Geophys. Res. 87, 4,657–4,667, 1982.

25 J. Verhoef and H.R. Jackson, Admittance signatures of rifted and transform margins: Examples from eastern Canada, Geophys. J. in press.

26 D.T. Sandwell, Thermomechanical evolution of oceanic fracture zones, J. Geophys. Res. 89, 11,401–11,413, 1984.

27 E.M. Parmentier and W.F. Haxby, Thermal stresses in the oceanic lithosphere: evidence from geoid anomalies at fracture zones, J. Geophys. Res. 91, 7193–7204, 1986.

28 W.F. Haxby and E.M. Parmentier, Thermal constraints and the state of stress in the oceanic lithosphere, J. Geophys. Res. 93, 6419–6429, 1988.

29 P. Wessel and W.F. Haxby, Thermal stresses, differential subsidence, and flexure at oceanic fracture zones, J. Geophys. Res. 95, 375–391, 1990.

30 M.I. Hetenyi, Beams on Elastic Foundations: Theory with Applications in the Fields of Civil and Mechanical Engineering, Univ. Mich. Sci. Ser. 16, 255 pp., 1979.

31 P. Barton and R. Wood, Tectonic evolution of the North Sea basin: crustal stretching and subsidence, Geophys. J.R. Astron. Soc. 79, 987–1022, 1984.

32 A.B. Watts, Gravity anomalies, crustal structure and flexure of the lithosphere at the Baltimore Canyon Trough, Earth Planet. Sci. Lett. 89, 221–238, 1988.

33 C. Beaumont, C.E. Keen and R. Boutilier, On the evolution of rifted continental margins: Comparison of models and observations for the Nova Scotia margin, Geophys. J. R. Astron. Soc. 70, 667–715, 1982.

34 S. Fowler and D. McKenzie, Gravity studies of the Rockall and Exmouth Plateaux using SEASAT altimetry, Basin Res. 2, 27–34, 1989.

35 E. Blarez and J. Mascle, Shallow structures and evolution of the Ivory Coast and Ghana transform margin, Mar. Pet. Geol. 5, 54–64, 1988.

36 B.J. Todd, I. Reid and C.E. Keen, Crustal structure across the southwest Newfoundland transform margin, Can. J. Earth Sci. 25, 744–759, 1988.

37 I. Reid, Crustal structure beneath the southern Grand Banks: seismic refraction results and their implications, Can. J. Earth Sci. 25, 760–772, 1988.
38 C.E. Keen, W.A. Kay and W.R. Roest, Crustal anatomy of a transform continental margin, Tectonophysics 173, 527–544, 1990.
39 N.F. Exon and J.B. Willcox, Mesozoic outcrops on the lower continental slope off Exmouth, Western Australia, BMR J. Aust. Geol. Geophys. 1, 205–209, 1976.
40 A.J. Wright and T.J. Wheatley, Trapping mechanisms and the hydrocarbon potential of the Exmouth Plateau, western Australia, Aust. Pet. Explor. Assoc. J. 19, 19–29, 1979.
41 P.M. Barber, Paleotectonic evolution and hydrocarbon genesis of the central Exmouth Plateau, Aust. Pet. Explor. Assoc. J. 22, 131–144, 1982.
42 R.L. Larson, Early Cretaceous breakup of Gondwanaland off Western Australia, Geology 5, 57–60, 1977.
43 D.V. Kent and F.M. Gradstein, A Jurassic to recent chronology, in: The Western North Atlantic Region, Geology of North America, vol. M, P.R. Vogt and B.E. Tucholke, eds., Geological Society of America, Boulder, Colo., 1986.
44 B.U. Haq, U. von Rad, S. O'Connell et al., Proc. ODP, Init. Results 122, 1990.
45 J.C. Mutter, R.L. Larson, P. Buhl, J.B. Diebold, J. Alsop, J. Lorenzo, R. Mithal, J. Hopper, D. Falvey, P. Williamson and F. Brassil, Extension of the Exmouth Plateau, offshore northwestern Australia: deep seismic reflection/refraction evidence for simple and pure shear mechanisms, Geology 17, 15–18, 1989.
46 J.J. Veevers and M.H. Johnstone, Comparative stratigraphy and structure of the Western Australian margin and the adjacent deep ocean floor, Init. Rep. DSDP 27, 571–585, 1974.
47 A.W. Bally, D. Bernoulli, G.A. Davis and L. Montadert, Listric normal faults, Oceanol. Acta. 4, 87–101, 1981.
48 B. Wernicke and B.C. Burchfiel, Modes of extensional tectonics, J. Struct. Geol. 4, 105–115, 1982.
49 A.D. Gibbs, Structural evolution of extensional basin margins, J. Geol. Soc. London 141, 609–620, 1984.
50 M.G. Langseth and M.A. Hobart, Interpretation of heat flow measurements in the Vema Fracture Zone, Geophys. Res. Lett. 3, 241–244, 1976.
51 K.E. Louden and D.W. Forsyth, Thermal conduction across fracture zones and the gravitational edge effect, J. Geophys. Res. 81, 4,869–4,874, 1976.
52 Y. Chen, Thermal models of oceanic transform faults, J. Geophys. Res. 93, 8,839–8,851, 1988.
53 L.G. Fullerton, W.W. Sager and D.W. Handschumacher, Late Jurassic–Early Cretaceous evolution of the eastern Indian Ocean adjacent to northwest Australia, J. Geophys. Res. 94, 2937–2953, 1989.
54 I.G. Omar, M.S. Steckler, W.B. Buck and B.P. Kohn, Fission-track analysis of basement apatites at the western margin of the Gulf of Suez rift, Egypt: evidence for synchroneity of uplift and subsidence, Earth Planet. Sci. Lett. 94, 316–328, 1989.
55 R.W. Buck, Small-scale convection induced by passive rifting: the cause for uplift of rift shoulders, Earth Planet. Sci. Lett. 77, 362–372, 1986.
56 P. Londsdale, A transform continental margin rich in hydrocarbons, A.A.P.G. Bull. 69, 1160–1180, 1985.
57 N.F. Exon and J.B. Willcox, The Exmouth Plateau, stratigraphy, structure and petroleum potential, Aust. Bur. Miner. Res. Geol. Geophys. Bull. 199, 1–52, 1980.